

Article

Event-Triggered Synchronization of Coupled Neural Networks with Reaction–Diffusion Terms

Abulajiang Aili ^{1,*}, Shenglong Chen ²  and Sibao Zhang ¹

¹ School of Mathematics and Statistics, Kashi University, Kashi 844006, China; zhangsibao@ksu.edu.cn

² College of Mathematics and System Science, Xinjiang University, Urumqi 830017, China; slchen@stu.xju.edu.cn

* Correspondence: abuali@ksu.edu.cn

Abstract: This paper focuses on the event-triggered synchronization of coupled neural networks with reaction–diffusion terms. At first, an effective event-triggered controller was designed based on time sampling. It is worth noting that the data of the controller for this type can be updated only when corresponding triggering conditions are satisfied, which can significantly reduce the communication burden of the control systems compared to other control strategies. Furthermore, some sufficient criteria were obtained to ensure the event-triggered synchronization of the considered systems through the use of an inequality techniques as well as the designed controller. Finally, the validity of the theoretical results was confirmed using numerical examples.

Keywords: synchronization; coupled neural networks; event-triggered control; reaction–diffusion terms

MSC: 34D20; 34H05; 93B52; 93C20



Citation: Aili, A.; Chen, S.; Zhang, S. Event-Triggered Synchronization of Coupled Neural Networks with Reaction–Diffusion Terms.

Mathematics **2024**, *12*, 1409. <https://doi.org/10.3390/math12091409>

Academic Editor: Carlos E. Castañeda

Received: 29 March 2024

Revised: 25 April 2024

Accepted: 2 May 2024

Published: 4 May 2024



Copyright: © 2024 by the authors. Licensee MDPI, Basel, Switzerland. This article is an open access article distributed under the terms and conditions of the Creative Commons Attribution (CC BY) license (<https://creativecommons.org/licenses/by/4.0/>).

1. Introduction

In recent decades, as a crucial nonlinear dynamic system that can effectively imitate the speciality of animal neurons and implement distributed parallel information processing, neural networks (NNs) have widespread applications in many fields including character recognition and optimal control [1–3]. In view of NNs' high-nonlinearity and fine fault tolerance, the dynamics of NNs of various sorts have been investigated, such as competitive NNs [4,5], BAM NNs [6], inertial NNs [7], fuzzy NNs [8,9], memristive NNs [10,11] and coupled NNs [12]. Therefore, coupled NNs (CNNs) can be seen as extremely special, complex NNs composed of numerous nodes interconnected together, which have not only the excellent properties of classical single NNs but also the abilities to perform all kinds of intricate missions in practice. Consequently, it is of important theoretical and practical significance to study the dynamics of CNNs, and some valuable results associated with them have been obtained [12–15]. For example, in [12], bipartite synchronization was investigated for CNNs with uncertain parameters by designing a discontinuous control and a periodically intermittent one. Selvaraj et al. analyzed the synchronization control of stochastic CNNs under the influence of Markovian switching as well as input saturation [13]. According to differential inequality and Lyapunov theory, cluster synchronization was explored for delayed CNNs in [14]. Luo et al. dealt with the synchronization problem of memristor-based CNNs and obtained some new criteria that are easy to complement [15].

It is worth noting that the aforementioned works about NNs only paid attention to the time factor but ignored the space one. In other words, the reaction–diffusion mechanism was not considered. In reality, when electrons shift in the electromagnetic field with asymmetrically nonhomogeneous speciality, the spatial diffusion effect is inevitable. Moreover, there are a large number of reaction–diffusion phenomena in many disciplines, especially

in the fields of chemistry and biology. For example, reaction–diffusion phenomena occur through the interactions of substances in various chemical reactions. Since the traditional artificial NNs are realized by means of electronic circuits, it is of great meaning and necessity to analyze NNs with reaction–diffusion terms. Up to now, numerous remarkable achievements with respect to reaction–diffusion neural networks (R-DNNs) have been reported, such as in [16–22].

At present, there are some interesting results with regard to the dynamical behaviors of coupled R-DNNs (CR-DNNs) through the combination of CNNs and R-DNNs [23–30]. For instance, by proposing a novel passivity definition and using an inequality technique, Wang et al. derived some valuable passivity and dissipativity criteria for CR-DNNs [23]. Lu et al. considered the exponential synchronization of CR-DNNs and obtained some easily verified and new conditions by developing a generalized intermittent control method [28]. By virtue of Lyapunov’s approach, Wu et al. dealt with the synchronization issue of CR-DNNs and yielded some sufficient criteria using an impulsive pinning approach [29]. In [30], Lin et al. analyzed the pinning synchronization of CR-DNNs and provided some interesting results with the help of NLEVec and a designed controller.

Among the above dynamics, synchronization is one of the most crucial and significant ones, which can be reflected in its vital theoretical value and various kinds of potential applications involving information processing as well as secure communication. However, NNs cannot realize synchronization by themselves due to the influence of external disturbances; consequently, some effective control strategies have been proposed by scholars for the past few years, including but not limited to feedback control [31], sample-data control [32], quantized control [33,34], pinning control [35], impulsive control [36], adaptive control [37,38], aperiodically switching control [39] and event-triggered control [40–43], of which event-triggered control is a very effective control strategy; it can overcome the high cost caused by continuous control and reduce the frequency of data updates and the number of communications. In [44], Jin et al. investigated the finite-time synchronization of delayed semi-markov NNs by designing an event-triggered scheme. In [45], Vadivel et al. dealt with the strict dissipativity synchronization problem of static NNs under an event-triggered scheme. The robust synchronization was analyzed for master–slave NNs based on an event-triggered control method in [46]. The synchronization problem of inertial NNs was addressed by means of an event-triggered control approach in [47]. To the best of our knowledge, there is still very little work on the event-triggered control-based synchronization of CR-DNNs so far, which motivates us to carry out further research.

Based on the above analysis and discussion, the primary task was to explore for the event-triggered synchronization of CR-DNNs in this study. The cardinal contents and contributions of this study are listed as follows:

- (1) A class of CR-DNNs model is established, and an effective event-triggered controller is designed based on time sampling.
- (2) Some sufficient criteria are obtained to ensure the event-triggered synchronization of CR-DNNs, which are composed of several linear matrix inequalities.
- (3) The effectiveness of the event-triggered strategy and theoretical results are verified using numerical examples.

The rest of this paper is organized as follows. In Section 2, the model of CR-DNNs is presented, and some requisite lemmas are introduced. In Section 3, the event-triggered synchronization criteria are provided, obtained by designing a concise controller. Some numerical examples are presented to demonstrate the feasibility of the obtained results in Section 4. Finally, Section 5 provides the conclusion.

Notations: Let \mathbb{N} , \mathbb{R} and \mathbb{R}^+ denote the sets of natural numbers, real numbers and non-negative real numbers, respectively. A^T stands for the transpose of matrix A , and \otimes is the Kronecker product. \mathbb{R}^n and $\mathbb{R}^{n \times m}$ represent, respectively, an n -dimensional Euclidean space and a set of real matrices with order $n \times m$. $P > 0$ means that matrix P is a positive definite matrix, and I denotes the identity matrix with suitable dimensions. $\|\cdot\|$ is the Euclidean norm, and $Diag(\cdot)$ stands for the diagonal matrix. Furthermore, $(x_i)_{i=1}^n = (x_1, x_2, \dots, x_n)^T$,

$0_n=(0,0,\dots,0)^T$ and $\Omega=\{x=(x_1,x_2,\dots,x_m)^T \in \mathbb{R}^m : |x_l| \leq M_l, l=1,2,\dots,m\}$, where $M_l \in \mathbb{R}^+$.

2. Preliminaries and Model Description

In this section, we refer to [34] to consider CR-DNN model described by the following partial differential equation:

$$\frac{\partial u_r(t,x)}{\partial t} = \sum_{l=1}^m d_r \frac{\partial^2 u_r(t,x)}{\partial x_l^2} - a_r u_r(t,x) + \sum_{j=1}^n b_{rj} f(u_j(t,x)) + J_r, \tag{1}$$

where $x=(x_1,x_2,\dots,x_m)^T \in \Omega$ is the space vector; $t \in \mathbb{R}^+$ denotes the time variable; $r=1,2,\dots,n$, where n represents the number of neurons; $u_r(t,x)$ is the state variable of the r th neuron; the constant $d_r \geq 0$ stands for the diffusion coefficient of the r th neuron, a_r represents the rate at which the potential of the r th neuron resets to rest when the network is disconnected from the external input; b_{rj} is the connection strength between the j th neuron and the r th neuron; and the external bias is denoted by J_r .

The boundary and initial conditions for CR-DNN (1) are as follows:

$$\begin{aligned} u_r(t,x) &= 0, & (t,x) &\in \mathbb{R}^+ \times \partial\Omega. \\ u_r(0,x) &= \phi_r(x), & x &\in \Omega, \quad r=1,2,\dots,n. \end{aligned}$$

Assumption 1. Let the activation function $f_j(\cdot)$ satisfy the Lipschitz condition; that is, for any $\xi_1, \xi_2 \in \mathbb{R}$, there exists a constant a_j such that

$$|f_j(\xi_1) - f_j(\xi_2)| \leq a_j |\xi_1 - \xi_2|, \quad j=1,2,\dots,n.$$

For convenience, CR-DNNs (1) can be written in the following vector form

$$\frac{\partial u(t,x)}{\partial t} = D \sum_{l=1}^m \frac{\partial^2 u(t,x)}{\partial x_l^2} - Au(t,x) + Bf(u(t,x)) + J, \tag{2}$$

where $A = \text{diag}(a_1, a_2, \dots, a_n)$, $D = \text{diag}(d_1, d_2, \dots, d_n)$, $B = (b_{ij})_{n \times n}$, $J = \text{diag}(J_1, J_2, \dots, J_n)$ and $f(u(t,x)) = (f_r(u_r(t,x)))_{r=1}^n$.

The following linear CR-DNNs can be obtained by coupling (2) with the number of N :

$$\begin{aligned} \frac{\partial w_i(t,x)}{\partial t} &= D \sum_{l=1}^m \frac{\partial^2 w_i(t,x)}{\partial x_l^2} - Aw_i(t,x) + Bf(w_i(t,x)) + J \\ &+ C \sum_{j=1}^N g_{ij} \Gamma w_j(t,x) + v_i(t,x), \quad i=1,2,\dots,N, \end{aligned} \tag{3}$$

where $w_i(t,x) \in \mathbb{R}^n$ is the state vector of the i th node, $v_i(t,x)$ stands for the controller to be designed; $\Gamma \in \mathbb{R}^{n \times n}$ denotes the internal coupling matrix, and $G = (g_{ij})_{N \times N} \in \mathbb{R}^{N \times N}$ represents the external coupling matrix. If nodes i and $j(j \neq i)$ are connected to each other, then $g_{ij} \neq 0$, or $g_{ij} = 0$. In addition, the diagonal elements of G are

$$g_{ii} = - \sum_{j=1, j \neq i}^N g_{ij}, \quad i=1,2,\dots,N.$$

The boundary conditions and initial conditions of the CR-DNNs (3) are as follows:

$$w_i(t,x) = 0_n, \quad (t,x) \in \mathbb{R}^+ \times \partial\Omega, \tag{4}$$

$$w_i(0,x) = \Psi_i(x), \quad x \in \Omega \quad i=1,2,\dots,N, \tag{5}$$

where $\Psi_i(x)$ is a continuous function on Ω .

Let $\bar{W}(t, x) = \frac{1}{N} \sum_{i=1}^N w_i(t, x)$. Since $\sum_{i=1}^N \sum_{j=1}^N g_{ij} \Gamma w_j(t, x) = \sum_{i=1}^N (\sum_{j=1}^N g_{ij}) \Gamma w_j(t, x) = 0$, then it can follow from (3) that

$$\begin{aligned} \frac{\partial \bar{w}(t, x)}{\partial t} = & D \sum_{l=1}^m \frac{\partial^2 \bar{w}(t, x)}{\partial x_l^2} - A \bar{w}(t, x) \\ & + \frac{1}{N} B \sum_{l=1}^N f(w_l(t, x)) + J + \frac{1}{N} \sum_{l=1}^N v_l(t, x), \end{aligned} \tag{6}$$

where $i = 1, 2, \dots, N$.

Set $e_i(t, x) = w_i(t, x) - \bar{w}(t, x)$. Then, we have $\sum_{i=1}^N e_i(t, x) = 0$. There exist sampling times $0 = t_0 < t_1 < \dots < t_q < \dots$ such that $\lim_{q \rightarrow \infty} t_q = \infty, 0 < \underline{\tau} \leq t_{q+1} - t_q \leq \bar{\tau}$, where $\underline{\tau}$ and $\bar{\tau}$ are two positive numbers. Let $e_i(t_{q-1}^i, x)$ be the error sample value that the i th node sent to the controller most recently at time t_{q-1} . If the following inequality holds, then the latest sampled value $e_i(t_q, x)$ is transmitted to the controller at time t_q :

$$\|e_i(t_{q-1}^i, x) - e_i(t_q, x)\| > \beta_i \|e_i(t_{q-1}, x)\|, \quad \beta_i > 0, \tag{7}$$

where

$$e_i(t_q^i, x) = \begin{cases} e_i(t_q, x), & \text{If (7) holds,} \\ e_i(t_{q-1}^i, x), & \text{If (7) does not hold,} \end{cases}$$

and $e_i(t_0^i, x) = e_i(t_0, x)$.

The controller $v_i(t, x)$ was designed as follows:

$$v_i(t, x) = -K e_i(t_q^i, x), \quad i = 1, 2, \dots, N, \tag{8}$$

where $K = \text{diag}(K_1, K_2, \dots, K_n)$ is the control gain matrix. Therefore, the error system can be expressed as follows:

$$\begin{aligned} \frac{\partial e_i(t, x)}{\partial t} = & D \sum_{l=1}^m \frac{\partial^2 e_i(t, x)}{\partial x_l^2} - A e_i(t, x) + B f(e_i(t, x)) \\ & - \frac{B}{N} \sum_{i=1}^N f(w_i(t, x)) + C \sum_{j=1}^N g_{ij} \Gamma e_j(t, x) \\ & + K e_i(t_q^i, x) + \frac{1}{N} \sum_{i=1}^N v_i(t, x), \end{aligned} \tag{9}$$

where $i = 1, 2, \dots, N$.

Remark 1. In order to achieve the system control goal, many effective controllers were designed, and a great deal of valuable results were derived. For example, in [48], based on the Lyapunov method, the sliding mode control strategy was proposed to analyze the leader-following consensus issue. Sun et al. investigated the synchronization of nonlinear systems using an event-triggered control method [49]. Notably, the event-triggered control can not only reduce control cost but also decrease the communication times in the network compared with other control methods.

Define the artificial time delay $\tau(t) = t - t_q$, where $t_q \leq t \leq t_{q+1}$. Then, $\dot{\tau}(t) = 1, 0 \leq \tau(t) \leq \bar{\tau}$. Let trigger error $z_i(t_q, x) = e_i(t_q^i, x) - e_i(t_q, x)$. Then, one has

$$e_i(t_q^i, x) = z_i(t_q, x) + e_i(t_q, x) = z_i(t - \tau(t), x) + e_i(t - \tau(t), x).$$

Furthermore, we have

$$\begin{aligned} \frac{\partial e_i(t, x)}{\partial t} = & D \sum_{l=1}^m \frac{\partial^2 e_i(t, x)}{\partial x_l^2} - A e_i(t, x) + B f(e_i(t, x)) \\ & - \frac{B}{N} \sum_{i=1}^N f(w_i(t, x)) + C \sum_{j=1}^N g_{ij} \Gamma e_j(t, x) \\ & + K [z_i(t_k, x) + e_i(t - \tau(t), x)] + \frac{1}{N} \sum_{i=1}^N v_i(t, x), \end{aligned} \tag{10}$$

where $i = 1, 2, \dots, N$.

It follows from (7) that

$$z_i(t_q, x) = \begin{cases} 0, & \text{If (7) holds,} \\ e_i(t_{q-1}^i, x) - e_i(t_q, x), & \text{If (7) dose not hold.} \end{cases}$$

Whether (7) is true or not, the following inequality always holds:

$$\|z_i(t - \tau(t), x)\| = \|z_i(t_q, x)\| \leq \beta_i \|e_i(t_{q-1}, x)\| = \beta_i \|e_i(t - \tau(t), x)\|. \tag{11}$$

Let $e(t, x) = (e_1^T(t, x), e_2^T(t, x), \dots, e_N^T(t, x))^T$, $z(t_q, x) = (z_i(t_q, x))_{i=1}^N$, $w(t, x) = (w_1^T(t, x), w_2^T(t, x), \dots, w_N^T(t, x))^T$, $1_N = (1, 1, \dots, 1)_N^T$, $\hat{f}(t, x) = f(w_i(t, x)) - f(\bar{w}(t, x))$, $\hat{f}(e(t, x)) = c(\hat{f}(e(t, x)))_{i=1}^N$ and $F(t, x) = Bf(\bar{w}(t, x)) - \frac{B}{N} \sum_{i=1}^N f(w_i(t, x)) + \frac{1}{N} + \frac{1}{N} \sum_{i=1}^N v_i(t, x)$. Then, the error system can be written as

$$\begin{aligned} \frac{\partial e(t, x)}{\partial t} = & \sum_{l=1}^m (I_N \otimes D) \frac{\partial^2 e(t, x)}{\partial x_l^2} - (I_N \otimes A) e(t, x) + (I_N \otimes B) \bar{f}(e(t, x)), \\ & + C(G \otimes \Gamma) e(t, x) + (I_N \otimes K) [z(t_q, x) - e(t - \tau(t), x)] + 1_N \otimes F(t, x). \end{aligned} \tag{12}$$

A block diagram of the control mechanism is depicted by Figure 1.

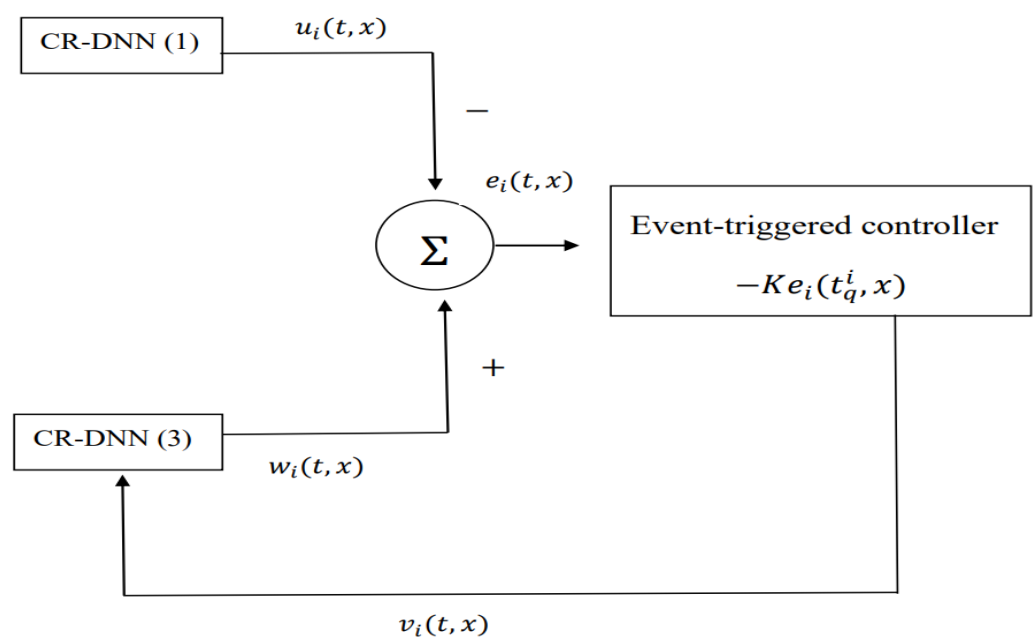


Figure 1. Block diagram of controller (8).

Definition 1. If $\lim_{t \rightarrow +\infty} \|w_i(t, x) - w_j(t, x)\| = 0, i, j = 1, 2, \dots, N$, then CR-DNNs (3) and (6) can achieve synchronization, where $w_i(t, x)$ is the solution of CR-DNN (3) satisfying boundary condition (4) and initial condition (5).

Next, in order to obtain the main results, the following lemmas are introduced.

Lemma 1 ([50]). For any vectors x and y and positive definite matrix P with appropriate dimensions, the following inequality holds

$$2x^T y \leq \frac{1}{\gamma} x^T P x + \gamma y^T P y, \quad \gamma > 0.$$

Lemma 2 ([51]). If $\omega(x)$ is a vector function, and $\hat{D} \in \mathbb{R}^{n \times n}$ satisfies $\hat{D} \geq 0$, then

$$\int_{\Omega} \omega^T(x) \hat{D} \omega(x) dx \leq \frac{4l_p^2}{\pi^2} \int_{\Omega} \frac{\partial \omega^T}{\partial x_p} \hat{D} \frac{\partial \omega}{\partial x_p} dx,$$

where $\omega(x)|_{\partial\Omega} = 0_n$.

Lemma 3 (Jensen’s inequality) [52]. Let $E \subset \mathbb{R}^m$ and $\omega : E \rightarrow \mathbb{R}^n$ be a measurable set and a vector function. Then, for any n -order matrix $R \geq 0$, one has

$$\mu(E) \int_E \omega^T R \omega d\mu \geq \int_E \omega^T d\mu R \int_E \omega d\mu,$$

where $0 < \mu(E) < \infty$.

Lemma 4 ([53]). For any integers $m, n, a_i > 0$, if $f_i : \mathbb{R}^m \rightarrow \mathbb{R}$ is a positive function, and $g_{ij} : \mathbb{R}^m \rightarrow \mathbb{R}$ is positive in an open subset D of \mathbb{R}^m , then we have

$$\min_{a_i} \sum_{i=1}^n \frac{1}{a_i} f_i = \sum_{i=1}^n f_i + \max_{g_{ij}} \sum_{i=1}^n \sum_{i=1, j \neq i}^n g_{ij},$$

where $\sum_{i=1}^n a_i = 1$, and $\begin{bmatrix} f_i & g_{ij} \\ g_{ij} & f_j \end{bmatrix} \geq 0$, where $i, j = 1, 2, \dots, n$.

Lemma 5 ([54]). If there is a field U containing a distant point and a positive (negative) definite function $V(x)$ such that $\frac{dV(t)}{dt}$ is semi-negative (positive) definite, then the zero solution of system $\frac{dx}{dt} = f(x), f(0) = 0$ is stable, and the zero solution of system $\frac{dx}{dt} = f(x), f(0) = 0$ is asymptotically stable when $\frac{dV(t)}{dt}$ is negative (positive) definite.

3. Main Results

In this section, some sufficient conditions are obtained to guarantee the synchronization of CR-DNNs (3) and (6) based on the event-based control strategy (8).

Theorem 1. Under Assumption 1, CR-DNNs (3) and (6) can achieve synchronization if there exist n -order symmetric matrices \tilde{K} and $P_1 > 0, P_2 > 0, P_3 > 0$ and $P_4 > 0$ such that

$$\begin{pmatrix} P_3 & \tilde{K} \\ \tilde{K} & P_3 \end{pmatrix} \geq 0, \tag{13}$$

$$\Lambda < 0, \tag{14}$$

where $\Lambda = \{\Lambda_{ij}\}$ is a symmetric block matrix consisting of the following matrices: $\Lambda_{11} = -\sum_{l=1}^m \frac{\phi^2}{4M_l} I_N \otimes (p_1 D + D P_1) - 2(I_N \otimes A) + C(G \otimes (P_1 \Gamma + \Gamma P_1)) + I_N \otimes P_2 - I_N \otimes P_3 + I_N \otimes$

$L, \Lambda_{12} = I_N \otimes (P_3 - \tilde{K} - P_1K), \Lambda_{13} = I_N \otimes \tilde{K}, \Lambda_{14} = -I_N \otimes AP_4 + C(G \otimes \Gamma P_4), \Lambda_{15} = I_N \otimes B, \Lambda_{16} = -I_N \otimes P_1K, \Lambda_{22} = [I_N \otimes (2\tilde{K} - 2P_3) + \Lambda \otimes I_n], \Lambda_{23} = I_N \otimes (P_3 - \tilde{K}), \Lambda_{24} = -I_N \otimes KP_4, \Lambda_{33} = -I_N \otimes p_2 - I_N \otimes P_3, \Lambda_{44} = \tilde{\tau}^2 I_N \otimes P_3 - 2I_N \otimes P_4, \Lambda_{45} = I_N \otimes P_4B, \Lambda_{46} = -I_N \otimes P_4K$ and $\Lambda_{55} = \Lambda_{66} = -I_{Nn}$.

Proof. Firstly, we define the Lyapunov function as follows:

$$V(t) = V_1(t) + V_2(t) + V_3(t) + V_4(t), \tag{15}$$

where

$$\begin{aligned} V_1(t) &= \int_{\Omega} e^T(t, x)(I_N \otimes P_1)e(t, x)dx, \\ V_2(t) &= \int_{\Omega} \int_{t-\tau(t)}^t e^T(s, x)(I_N \otimes P_2)e(s, x)dsdx, \\ V_3(t) &= \tilde{\tau} \int_{\Omega} \int_{-\tau}^0 \int_{t+\theta}^t \frac{\partial e^T(s, x)}{\partial s}(I_N \otimes P_3) \frac{\partial e(s, x)}{\partial s} dsd\theta dx, \\ V_4(t) &= \sum_{l=1}^m \int_{\Omega} \frac{\partial e^T(t, x)}{\partial x_l}(I_N \otimes P_4D) \frac{\partial e(t, x)}{\partial x_l}. \end{aligned}$$

For any $t \in [t_k, t_{k+1})$, calculating the derivative of $V_1(t)$ with respect to t along the trajectory of CR-DNN (12) yields

$$\begin{aligned} \frac{dV_1(t)}{dt} &= 2 \int_{\Omega} e^T(t, x)(I_N \otimes P_1) \frac{\partial e(t, x)}{\partial t} dx \\ &= 2 \int_{\Omega} e^T(t, x)(I_N \otimes P_1) \left\{ \sum_{l=1}^m (I_N \otimes D) \frac{\partial^2 e(t, x)}{\partial x_l^2} \right. \\ &\quad - (I_N \otimes A)e(t, x) + (I_N \otimes B)f(w(t, x)) \\ &\quad - (I_N \otimes B)f(u(t, x)) + C(G \otimes P)e(t, x) \\ &\quad \left. + (I_N \otimes K)[z(t_k, x) + e(t - \tau(t), x)] \right\} dx. \end{aligned} \tag{16}$$

Through using boundary condition (4), Green’s formula and Lemma 2, the following equation can be obtained:

$$\begin{aligned} &2 \int_{\Omega} \sum_{i=1}^m e^T(t, x)(I_N \otimes P_1)(I_N \otimes D) \frac{\partial^2 e(t, x)}{\partial x_l^2} dx \\ &= 2 \int_{\Omega} \sum_{i=1}^m e^T(t, x)(I_N \otimes P_1D) \frac{\partial^2 e(t, x)}{\partial x_l^2} dx \\ &= \int_{\Omega} e^T(t, x)(I_N \otimes P_1D) \sum_{l=1}^m \frac{\partial^2 e(t, x)}{\partial x_l^2} dx \\ &\quad + \left(\sum_{l=1}^m \frac{\partial^2 e(t, x)}{\partial x_l^2} \right)^T (I_N \otimes D^T P_1) e(t, x) dx \\ &= \int_{\Omega} e^T(t, x)(I_N \otimes P_1D + I_N \otimes D^T P_1) \sum_{l=1}^m \frac{\partial^2 e(t, x)}{\partial x_l^2} dx \\ &= \int_{\Omega} \sum_{l=1}^m \frac{\partial}{\partial x_l} \left[e^T(t, x)(I_N \otimes P_1D + I_N \otimes D^T P_1) \frac{\partial^T e(t, x)}{\partial x_l} \right] dx \\ &\quad - \int_{\Omega} \sum_{l=1}^m \frac{\partial^T e(t, x)}{\partial x_l} (I_N \otimes P_1D + I_N \otimes D^T P_1) \sum_{l=1}^m \frac{\partial e(t, x)}{\partial x_l} dx, \end{aligned} \tag{17}$$

due to

$$\int_{\Omega} \sum_{l=1}^m \frac{\partial}{\partial x_l} \left[e^T(t, x)(I_N \otimes P_1D + I_N \otimes D^T P_1) \frac{\partial^T e(t, x)}{\partial x_l} \right] dx = 0, \tag{18}$$

Then, we have

$$\begin{aligned}
 & - \int_{\Omega} \sum_{l=1}^m \frac{\partial^T e(t, x)}{\partial x_l} (I_N \otimes P_1 D + I_N \otimes D^T P_1) \sum_{l=1}^m \frac{\partial e(t, x)}{\partial x_l} dx \\
 & \leq - \sum_{l=1}^m \frac{\phi^2}{4M_l} \int_{\Omega} e^T(t, x) (I_N \otimes P_1 D + I_N \otimes D^T P_1) e(t, x) dx.
 \end{aligned} \tag{19}$$

Owing to

$$e^T(t, x) (I_N \otimes P_1) (1_N \otimes F(t, z)) = \sum_{i=1}^m e_i(t, x) P_1 F(t, x) = 0, \tag{20}$$

one has

$$\begin{aligned}
 \frac{dV_1(t)}{dt} & \leq \int_{\Omega} e^T(t, x) \left\{ - \sum_{l=1}^m \frac{\phi^2}{4M_l} I_N \otimes (P_1 D + D^T P_1) e(t, x) \right. \\
 & \quad - 2(I_N \otimes A) e(t, x) + 2(I_N \otimes B) F(e(t, x)) \\
 & \quad + C[G \otimes (P_1 \Gamma + \Gamma P_1)] e(t, x) \\
 & \quad \left. - [I_N \otimes (2P_1 K)] [z(t, x) + e(t - \tau(t), x)] \right\} dx.
 \end{aligned} \tag{21}$$

For $V_2(t)$, we have

$$\frac{dV_2(t)}{dt} = \int_{\Omega} e^T(t, x) (I_N \otimes P_2) e(t, x) dx - \int_{\Omega} e^T(t - \bar{\tau}, x) (I_N \otimes P_2) e(t - \bar{\tau}, x) dx. \tag{22}$$

It follows from Lemmas 3 and 4 that

$$\begin{aligned}
 & \bar{\tau} \int_{t-\bar{\tau}}^t \frac{\partial e^T(s, x)}{\partial s} (I_N \otimes P_3) \frac{\partial e(s, x)}{\partial s} ds \\
 & = \bar{\tau} \left(\int_{t-\bar{\tau}}^{t-\tau(t)} + \int_{t-\tau(t)}^t \right) \frac{\partial e^T(s, x)}{\partial s} (I_N \otimes P_3) \frac{\partial e(s, x)}{\partial s} ds \\
 & \geq \frac{\bar{\tau}}{\bar{\tau} - \tau(t)} \int_{t-\bar{\tau}}^{t-\tau(t)} \frac{\partial e^T(s, x)}{\partial s} ds (I_N \otimes P_3) \int_{t-\bar{\tau}}^{t-\tau(t)} \frac{\partial e(s, x)}{\partial s} ds \\
 & \quad + \frac{\bar{\tau}}{\tau(t)} \int_{t-\tau(t)}^t \frac{\partial e^T(s, x)}{\partial s} ds (I_N \otimes P_3) \int_{t-\tau(t)}^t \frac{\partial e(s, x)}{\partial s} ds \\
 & \geq \int_{t-\bar{\tau}}^{t-\tau(t)} \frac{\partial e^T(s, x)}{\partial s} ds (I_N \otimes P_3) \int_{t-\bar{\tau}}^{t-\tau(t)} \frac{\partial e(s, x)}{\partial s} ds \\
 & \quad + \int_{t-\tau(t)}^t \frac{\partial e^T(s, x)}{\partial s} ds (I_N \otimes P_3) \int_{t-\tau(t)}^t \frac{\partial e(s, x)}{\partial s} ds \\
 & \quad + 2 \int_{t-\bar{\tau}}^{t-\tau(t)} \frac{\partial e^T(s, x)}{\partial s} ds (I_N \otimes \tilde{K}) \int_{t-\tau(t)}^t \frac{\partial e(s, x)}{\partial s} ds,
 \end{aligned} \tag{23}$$

Therefore,

$$\begin{aligned}
 \frac{dV_3(t)}{dt} & = \bar{\tau}^2 \int_{\Omega} \frac{\partial e^T(t, x)}{\partial s} (I_N \otimes P_3) \frac{\partial e(s, x)}{\partial s} dx \\
 & \quad - \bar{\tau} \int_{\Omega} \int_{-\bar{\tau}}^0 \frac{\partial e^T(t + \theta, x)}{\partial(t + \theta)} (I_N \otimes P_3) \frac{\partial e(t + \theta, x)}{\partial(t + \theta)} d\theta dx \\
 & = \bar{\tau}^2 \int_{\Omega} \frac{\partial e^T(t, x)}{\partial s} (I_N \otimes P_3) \frac{\partial e(s, x)}{\partial s} dx \\
 & \quad - \bar{\tau} \int_{\Omega} \int_{t-\bar{\tau}}^t \frac{\partial e^T(s, x)}{\partial s} (I_N \otimes P_3) \frac{\partial e(s, x)}{\partial s} d\theta ds dx,
 \end{aligned} \tag{24}$$

Then, we have

$$\begin{aligned} \frac{dV_3(t)}{dt} \leq & \int_{\Omega} \left\{ \frac{\partial e^T(t, x)}{\partial t} (\bar{\tau}^2 I_N \otimes P_3) \frac{\partial e(t, x)}{\partial t} \right. \\ & - [e^T(t - \tau(t), x) - e^T(t - \bar{\tau}, x)] (I_N \otimes P_3) [e(t - \tau(t), x) - e(t - \bar{\tau}, x)] \\ & - [e^T(t, x) - e^T(t - \tau(t), x)] (I_N \otimes P_3) [e(t, x) - e(t - \tau(t), x)] \\ & \left. - 2[e^T(t - \tau(t), x) - e^T(t - \bar{\tau}, x)] (I_N \otimes \tilde{K}) [e(t, x) - e(t - \tau(t), x)] \right\}. \end{aligned} \tag{25}$$

For $V_4(t)$, we have

$$\frac{dV_4(t)}{dt} = 2 \sum_{l=1}^m \int_{\Omega} \frac{\partial e^T(t, x)}{\partial x_l} (I_N \otimes P_4 D) \frac{\partial^2 e(t, x)}{\partial x_l \partial t} dx. \tag{26}$$

It is easy to show that

$$\begin{aligned} & 2 \int_{\Omega} \frac{\partial e^T(t, x)}{\partial t} (I_N \otimes P_4) \frac{\partial e(t, x)}{\partial t} dx \\ + & 2 \int_{\Omega} \frac{\partial e^T(t, x)}{\partial t} (I_N \otimes P_4) \sum_{l=1}^m (I_N \otimes D) \frac{\partial^2 e(t, x)}{\partial x_l^2} dx \\ - & 2 \int_{\Omega} \frac{\partial e^T(t, x)}{\partial t} (I_N \otimes P_4) \{ (I_N \otimes A) e(t, x) \\ - & (I_N \otimes B) \hat{f}(e(t, x)) - C(G \otimes \Gamma) e(t, x) \\ + & (I_N \otimes K) [z(t_q, x) + e(t - \tau(t), x)] - 1_N \otimes F(t, x) \} dx = 0, \end{aligned} \tag{27}$$

because of

$$\begin{aligned} & \sum_{l=1}^m \int_{\Omega} \frac{\partial e^T(t, x)}{\partial t} (I_N \otimes P_4) [I_N \otimes D] \frac{\partial^2 e(t, x)}{\partial x_l^2} dx \\ = & \int_{\Omega} \left(\frac{\partial e^T(t, x)}{\partial t} (I_N \otimes P_4 D) \frac{\partial e(t, x)}{\partial x_l} \right)_{p=1}^m \cdot \bar{n} ds \\ - & \int_{\Omega} \sum_{l=1}^m \frac{\partial^2 e^T(t, x)}{\partial t \partial x_p} (I_N \otimes P_4 D) \frac{e(t, x)}{\partial x_l} dx, \end{aligned} \tag{28}$$

and

$$\frac{\partial e^T(t, x)}{\partial t} (I_N \otimes P_4) 1_N \otimes F(t, x) = \frac{\partial}{\partial t} \sum_{l=1}^m e_l(t, x) P_4 F(t, x) = 0, \tag{29}$$

Then, we have

$$\begin{aligned} & - 2 \int_{\Omega} \frac{\partial e^T(t, x)}{\partial t} (I_N \otimes P_4) \frac{\partial e(t, x)}{\partial e_{x_l}} dx \\ - & 2 \int_{\Omega} \frac{\partial e^T(t, x)}{\partial t} \{ (I_N \otimes P_4) (I_N \otimes A) e(t, x) \\ - & (I_N \otimes B) \hat{f}(e(t, x)) - C(G \otimes \Gamma) e(t, x) \\ + & (I_N \otimes K) [z(t_q, x) + e(t - \tau(t), x)] \} dx \\ - & 2 \int_{\Omega} \sum_{l=1}^m \frac{\partial^2 e^T(t, x)}{\partial x_l \partial t} (I_N \otimes P_4 D) \frac{\partial e(t, x)}{\partial x_l} dx = 0. \end{aligned} \tag{30}$$

It can follow from (8) that

$$z^T(t_q, x) z(t_q, x) \leq e^T(t - \tau(t), x) (\Lambda \otimes I_N) e(t - \tau(t), x), \tag{31}$$

Then,

$$e^T(t - \tau(t), x) (\Lambda \otimes I_N) e(t - \tau(t), x) - z^T(t_q, x) z(t_q, x) \geq 0. \tag{32}$$

According to Assumption 1, one has

$$\hat{f}^T(e(t, x))\hat{f}(e(t, x)) \leq e^T(t, x)(I_N \otimes L)e(t, x), \tag{33}$$

That is

$$-\hat{f}^T(e(t, x))\hat{f}(e(t, x)) + e^T(t, x)(I_N \otimes L)e(t, x) \geq 0. \tag{34}$$

Setting

$$\Psi(t, x) = (e^T(t, x), e^T(t - \tau(t), x), e^T(t - \bar{\tau}, x), \frac{\partial e^T(t, x)}{\partial t}, \hat{f}^T(e(t, x)), z^T(t_q, x))^T, \tag{35}$$

and combining (16)–(35) yields

$$\frac{dV(t)}{dt} = \int \Omega \Psi^T(t, x) \Lambda \Psi(t, x) ds \leq 0.$$

Therefore, it follows from Lemma 5 that $\lim_{t \rightarrow \infty} V(t) = 0$, which is to say that the zero solution of error system (12) is asymptotically stable, i.e., $\lim_{t \rightarrow \infty} \|e_i(t, x)\| = 0$. Then, CR-DNNs (3) and (6) can realize synchronization. \square

Remark 2. The synchronization criteria were obtained in the form of a linear matrix inequality, which makes calculation more convenient and concise.

4. Numerical Simulations

In this section, an example is provided to verify the feasibility of the synchronization criteria and event-triggered strategy.

Example. Consider the following CR-DNN with five nodes:

$$\begin{cases} \frac{\partial w_i(t, x)}{\partial t} = D \sum_{l=1}^m \frac{\partial^2 w_i(t, x)}{\partial x_l^2} - A w_i(t, x) + B \tanh(w_i(t, x)) + J \\ \quad + C \sum_{j=1}^N g_{ij} \Gamma w_j(t, x) + v_i(t, x), \quad i = 1, 2, \dots, N, \end{cases} \tag{36}$$

where each node contains three neurons, $t \in [0, +\infty)$, $x \in (-5, 5)$, $w_i(t, x) = (w_{ij}(t, x))_{j=1}^3$, $\tanh(w_i(t, x)) = (\tanh(w_{ij}(t, x)))_{j=1}^3$, $v_i(t, x) = (v_{i1}(t, x), v_{i2}(t, x))^T$,

$$J = \begin{pmatrix} 1.2 & 0.7 & -4 \\ -1.6 & 2.8 & 0.5 \\ 1.5 & 1.7 & 1 \end{pmatrix}, \quad G = \begin{pmatrix} -0.1 & 0 & 0 & 0.1 & 0 \\ 0 & -0.2 & 0 & 0.2 & 0 \\ 0 & 0 & -0.4 & 0 & 0.4 \\ 0.1 & 0.2 & 0 & -0.5 & 0.2 \\ 0 & 0 & 0.4 & 0.2 & -0.6 \end{pmatrix},$$

and the values of the other parameters are shown in Table 1. $v_i(t, x)$ is event-triggered controller (8). Obviously, Assumption 1 is satisfied.

Let $z_i(t, x) = \frac{1}{5} \sum_{i=1}^5 w_i(t, x)$ and $e_i(t, x) = w_i(t, x) - z_i(t, x)$. The boundary conditions and initial conditions of CR-DNN (36) are as follows:

$$\begin{aligned} \varphi_1(x) &= (-0.6 \cos(0.4\pi x), \cos(0.4\pi x), \sin(0.4\pi x) + 0.6)^T, \\ \varphi_1(x) &= (-0.2x^2 + 0.4, -0.2x^2 - 1, 0.2x^2 - 1)^T, \\ \varphi_1(x) &= (-3, 3, -3)^T, \\ \varphi_1(x) &= (-1, -1, 1)^T, \\ \varphi_1(x) &= (0, 0, 0)^T, \quad x \in (-5, 5). \end{aligned}$$

Remark 3. According to the value of G , the coupling topology of CR-DNN (36) is shown in Figure 2, which reveals that (36) is connected. For when the control gain matrix K is a zero matrix, that is, without external control, the dynamic trajectories of errors $e_i(t, x)$ and $e_i(t, 0)$ are shown in Figures 3 and 4, which show that CR-DNN (36) cannot realize synchronization. In order to realize the synchronization goal, the sampling moment is selected as $t_q = 0.3q, q = 0, 1, 2, \dots, n$, $\beta = 0.5$ and control gain matrix $K = 6I_3$. \bar{K}, P_1, P_2 and P_3 can be obtained using the FEASP function in MATLAB. After simple calculations, the conditions of Theorem 1 are satisfied. Therefore, based on Theorem 1, CR-DNN (36) can achieve event-triggered synchronization, which is shown in Figures 5 and 6.

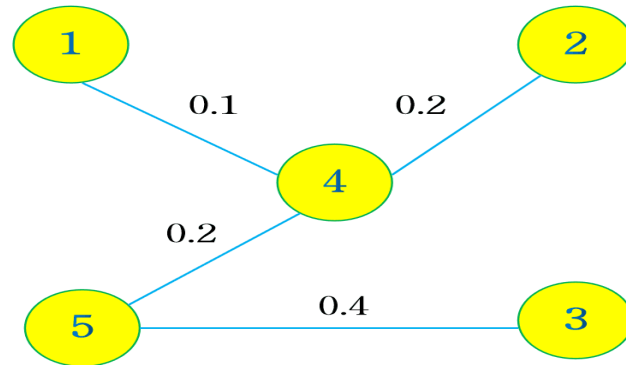


Figure 2. The coupling topology of CR-DNN (36).

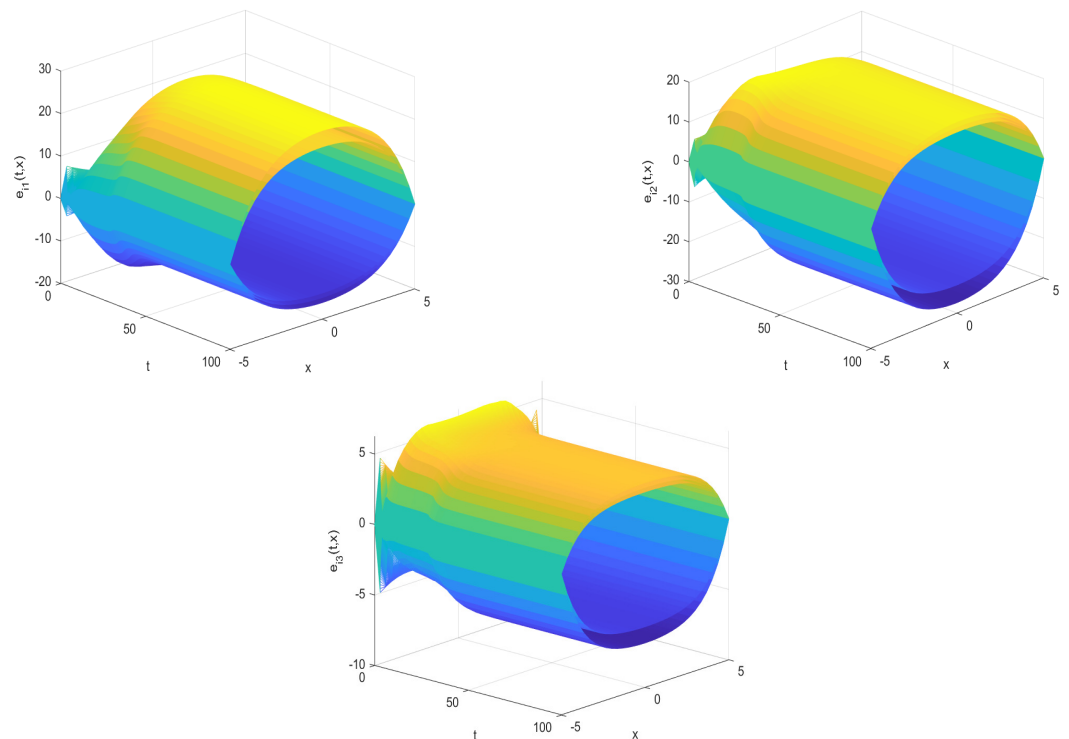


Figure 3. The dynamic trajectory of $e_i(t, x)$ when there is no control.

Table 1. The values of some parameters.

Parameter	Value	Parameter	Value
A	$\text{diag}(0.2,0.2,0.2)$	D	$\text{diag}(0.5,0.4,0.3)$
Γ	$\text{diag}(1,1,1)$	L	$\text{diag}(1,1,1)$
C	1		

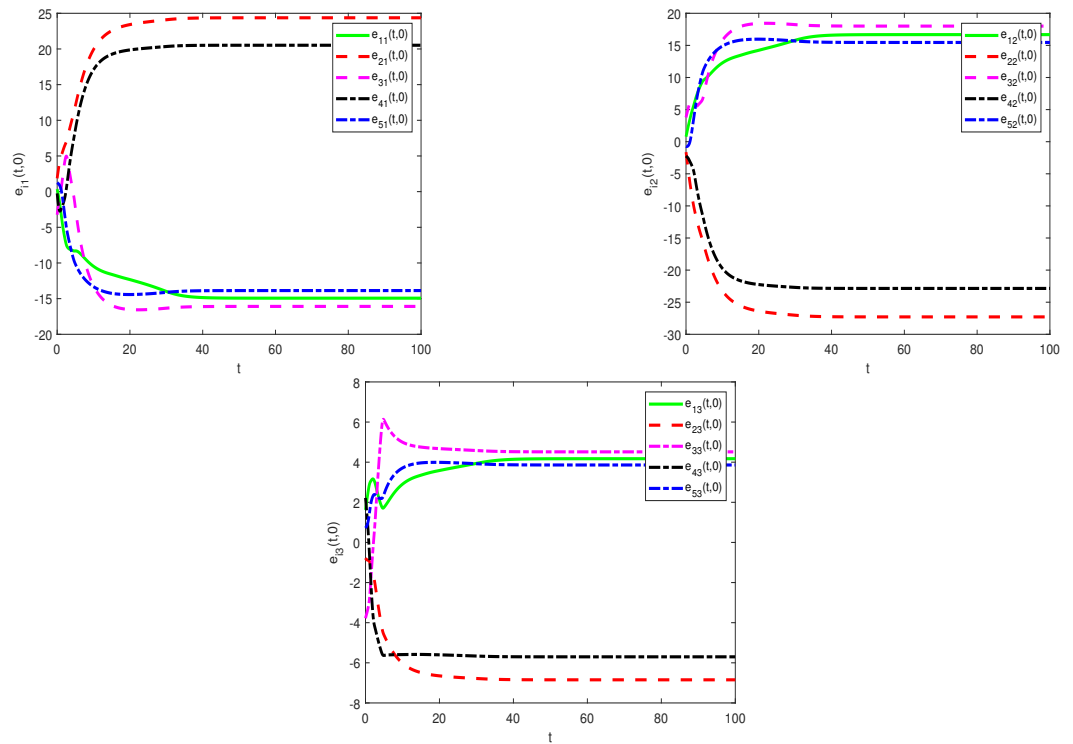


Figure 4. The dynamic trajectory of $e_i(t,0)$ when there is no control.

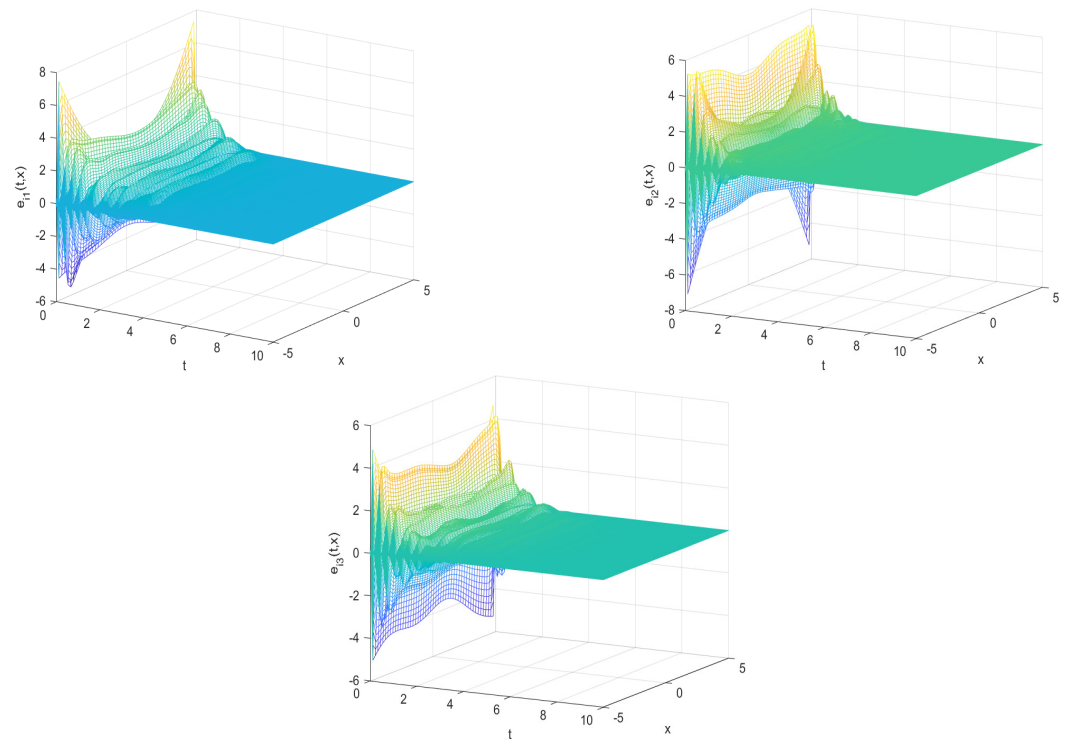


Figure 5. The time curves of $e_i(t,x)$ under event–triggered controller (8).

Remark 4. Currently, some interesting works have been conducted to discuss the influence of the parameters on synchronization [38,55,56]. For instance, Luo et al. [55] explored the influences of different triggering parameters and impulsive delays on the convergence rate. Chen et al. [38] considered the connection between the settling time and controller parameters. The research in [56] found that the faster the control gain, the faster the synchronization speed. Thus, in application, the values of the parameters can be adjusted according to actual needs.

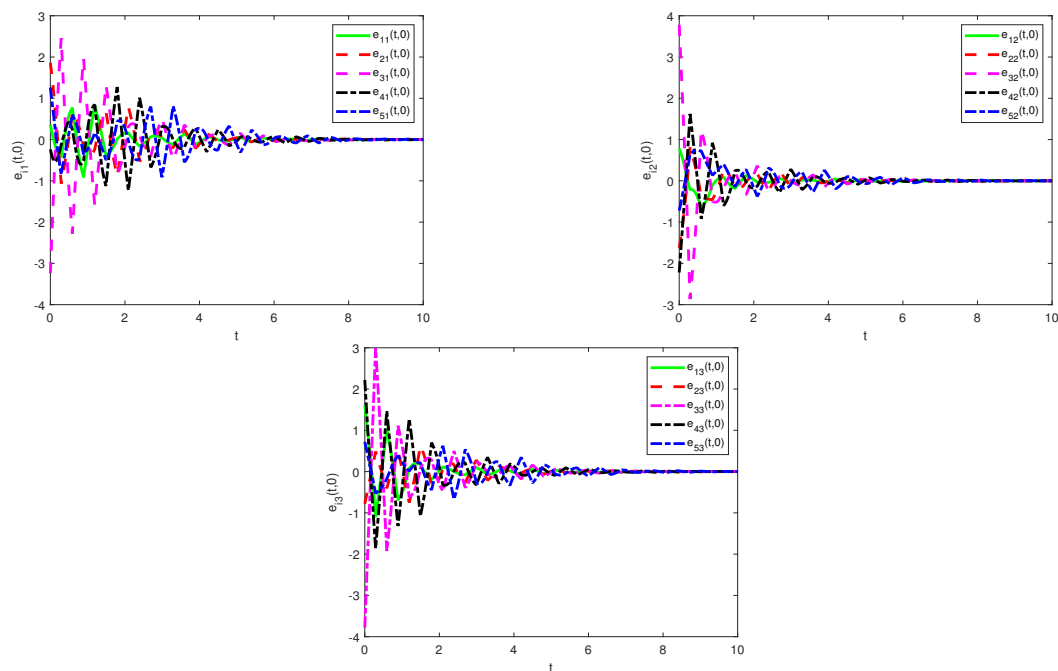


Figure 6. The time curves of $e_i(t, 0)$ under event-triggered controller (8).

5. Conclusions

In order to realize the event-triggered synchronization target of CR-DNNs, an effective event-triggering control strategy was designed in this study. At the same time, for the sake of avoiding the zero phenomenon, time sampling was conducted for the state variables of the CR-DNNs before judging the validity of the triggering conditions. In addition, in constructing appropriate Lyapunov functions, some sufficient conditions were obtained to ensure the synchronization of the CR-DNNs. In the end, numerical examples were provided to illustrate the feasibility of the obtained results.

The dynamics of a system with delay and stochastic effects have aroused widespread concern since they are unavoidable in practical application [57,58]. Therefore, the dynamical behaviors of CR-DNNs with delay and stochastic effects may be our future research priorities.

Author Contributions: A.A.: conceptualization, writing—original draft, funding acquisition and writing—review and editing. S.C.: formal analysis, writing—review and editing and funding acquisition. S.Z.: formal analysis and funding acquisition. All authors have read and agreed to the published version of the manuscript.

Funding: This work was supported by the 2023 School Scientific Research Project of Kashi University (Grant No. (2023)2857), the 2023 Annual Planning Project of the Commerce Statistical Society of China (Grant No. 2023STY61), the Innovation Project of Excellent Doctoral Students of Xinjiang University (Grant Nos. XJU2023BS017, XJU2024BS035), the Research Innovation Program for Postgraduates of Xinjiang Uygur Autonomous Region (Grant Nos. XJ2024G017, XJ2024G018, XJ2023G016, XJ2023G017), and the Natural Science Foundation of the Xinjiang Uygur Autonomous Region (Grant No. 2022D01A14).

Data Availability Statement: No new data were created or analyzed in this study. Data sharing is not applicable to this article.

Conflicts of Interest: The authors declare that they have no known competing financial interests or personal relationships that could have appeared to influence the work reported in this paper.

References

1. Humaidi, A.; Kadhim, T. Spiking versus traditional neural networks for character recognition on FPGA platform. *J. Telecommun. Electron. Comput. Eng.* **2018**, *10*, 109–115.
2. Luo, X.; Jiang, H.; Li, J.; Chen, S.; Xia, Y. Modeling and controlling delayed rumor propagation with general incidence in heterogeneous networks. *Int. J. Mod. Phys. C* **2024**, *35*, 2450020. [[CrossRef](#)]
3. Nasser, A.; Hasan, A.; Humaidi, A. DL-AMDet: Deep learning-based malware detector for android. *Intell. Syst. Appl.* **2024**, *21*, 200318. [[CrossRef](#)]
4. Pratap, A.; Raja, R.; Cao, J.; Rajchakit, G.; Fardoun, H. Stability and synchronization criteria for fractional order competitive neural networks with time delays: An asymptotic expansion of Mittag Leffler function. *J. Frankl. Inst.* **2019**, *356*, 2212–2239. [[CrossRef](#)]
5. Wang, L.; Zhang, C. Exponential synchronization of memristor-based competitive neural networks with reaction-diffusions and infinite distributed delays. *IEEE Trans. Neural Netw. Learn. Syst.* **2024**, *35*, 745–758. [[CrossRef](#)] [[PubMed](#)]
6. Chen, S.; Li, H.; Kao, Y.; Zhang, L.; Hu, C. Finite-time stabilization of fractional-order fuzzy quaternion-valued BAM neural networks via direct quaternion approach. *J. Frankl. Inst.* **2021**, *358*, 7650–7673. [[CrossRef](#)]
7. Yu, J.; Xiong, K.; Hu, C. Synchronization analysis for quaternion-valued delayed neural networks with impulse and inertia via a direct technique. *Mathematics* **2024**, *12*, 949. [[CrossRef](#)]
8. Wang, L.; Zeng, Z.; Ge, M. A disturbance rejection framework for finite-time and fixed-time stabilization of delayed memristive neural networks. *IEEE Trans. Syst. Man Cybern. Syst.* **2021**, *51*, 905–915. [[CrossRef](#)]
9. Chen, S.; Li, H.; Wang, L.; Hu, C.; Jiang, H.; Li, Z. Finite-time adaptive synchronization of fractional-order delayed quaternion-valued fuzzy neural networks. *Nonlinear Anal. Model. Control* **2023**, *28*, 804–823. [[CrossRef](#)]
10. Feng, L.; Hu, C.; Yu, J.; Jiang, H.; Wen, S. Fixed-time synchronization of coupled memristive complex-valued neural networks. *Chaos Solitons Fractals* **2021**, *148*, 110993. [[CrossRef](#)]
11. Wang, L.; He, H.; Zeng, Z. Global synchronization of fuzzy memristive neural networks with discrete and distributed delays. *IEEE Trans. Fuzzy Syst.* **2020**, *28*, 2022–2034. [[CrossRef](#)]
12. Mao, K.; Liu, X.; Cao, J.; Hu, Y. Finite-time bipartite synchronization of coupled neural networks with uncertain parameters. *Phys. A Stat. Mech. Its Appl.* **2022**, *585*, 126431. [[CrossRef](#)]
13. Selvaraj, P.; Sakthivel, R.; Kwon, O. Finite-time synchronization of stochastic coupled neural networks subject to Markovian switching and input saturation. *Neural Netw.* **2018**, *105*, 154–165. [[CrossRef](#)] [[PubMed](#)]
14. Zhang, X.; Li, C.; He, Z. Cluster synchronization of delayed coupled neural networks: Delay-dependent distributed impulsive control. *Neural Netw.* **2021**, *142*, 34–43. [[CrossRef](#)]
15. Luo, M.; Cheng, J.; Liu, X.; Zhong, S. An extended synchronization analysis for memristor-based coupled neural networks via aperiodically intermittent control. *Appl. Math. Comput.* **2019**, *344–345*, 163–182. [[CrossRef](#)]
16. Zhang, R.; Wang, H.; Park, J.; Lam, H.; He, P. Quasisynchronization of reaction-diffusion neural networks under deception attacks. *IEEE Trans. Syst. Man Cybern. Syst.* **2022**, *52*, 7833–7844. [[CrossRef](#)]
17. Stamov, G.; Stamova, I.; Martynyuk, A.; Stamov, T. Almost periodic dynamics in a new class of impulsive reaction-diffusion neural networks with fractional-like derivatives. *Chaos, Solitons Fractals* **2021**, *143*, 110647. [[CrossRef](#)]
18. Wang, Z.; Cao, J.; Cai, Z.; Tan, X.; Chen, R. Finite-time synchronization of reaction-diffusion neural networks with time-varying parameters and discontinuous activations. *Neurocomputing* **2021**, *447*, 272–281. [[CrossRef](#)]
19. Qin, Y.; Wang, J.; Chen, X.; Shi, K.; Shen, H. Anti-disturbance synchronization of fuzzy genetic regulatory networks with reaction-diffusion. *J. Frankl. Inst.* **2022**, *359*, 3733–3748. [[CrossRef](#)]
20. Hu, W.; Zhu, Q. Spatial-temporal dynamics of a non-monotone reaction-diffusion Hopfield's neural network model with delays. *Neural Comput. Appl.* **2022**, *34*, 11199–11212. [[CrossRef](#)]
21. Rao, R.; Huang, J.; Li, X. Stability analysis of nontrivial stationary solution and constant equilibrium point of reaction-diffusion neural networks with time delays under Dirichlet zero boundary value. *Neurocomputing* **2021**, *445*, 105–120. [[CrossRef](#)]
22. Mongolian, S.; Kao, Y.; Wang, C.; Xia, H. Robust mean square stability of delayed stochastic generalized uncertain impulsive reaction-diffusion neural networks. *J. Frankl. Inst.* **2021**, *358*, 877–894. [[CrossRef](#)]
23. Wang, J.; Wu, H.; Huang, T.; Ren, S.; Wu, J. Passivity analysis of coupled reaction-diffusion neural networks with dirichlet boundary conditions. *IEEE Trans. Syst. Man Cybern. Syst.* **2017**, *47*, 2148–2159. [[CrossRef](#)]
24. Cai, R.; Kou, C. Mittag-Leffler stabilization for coupled fractional reaction-diffusion neural networks subject to boundary-matched disturbance. *Math. Methods Appl. Sci.* **2023**, *46*, 3143–3156. [[CrossRef](#)]
25. Cao, Y.; Cao, Y.; Wen, S.; Huang, T.; Zeng, Z. Passivity analysis of coupled neural networks with reaction-diffusion terms and mixed delays. *J. Frankl. Inst.* **2018**, *355*, 8915–8933. [[CrossRef](#)]
26. Li, X.; Song, X.; Ning, Z.; Lu, J. Quasi-synchronization of hybrid coupled reaction-diffusion neural networks with parameter mismatches via time-space sampled-data control. *Int. J. Control Autom. Syst.* **2021**, *19*, 3087–3100. [[CrossRef](#)]
27. Cao, Y.; Kao, Y.; Park, J.; Bao, H. Global Mittag-Leffler stability of the delayed fractional-coupled reaction-diffusion system on networks without strong connectedness. *IEEE Trans. Neural Netw. Learn. Syst.* **2022**, *33*, 6473–6483. [[CrossRef](#)] [[PubMed](#)]
28. Lu, B.; Jiang, H.; Hu, C.; Abdurahman, A. Synchronization of hybrid coupled reaction-diffusion neural networks with time delays via generalized intermittent control with spacial sampled-data. *Neural Netw.* **2018**, *105*, 75–87. [[CrossRef](#)]

29. Wu, T.; Xiong, L.; Cao, J.; Park, J.; Cheng, J. Synchronization of coupled reaction-diffusion stochastic neural networks with time-varying delay via delay-dependent impulsive pinning control algorithm. *Commun. Nonlinear Sci. Numer. Simul.* **2021**, *99*, 105777. [[CrossRef](#)]
30. Lin, S.; Liu, X. Synchronization and control for directly coupled reaction-diffusion neural networks with multiple weights and hybrid coupling. *Neurocomputing* **2022**, *487*, 144–156. [[CrossRef](#)]
31. Chen, S.; Li, H.; Bao, H.; Zhang, L.; Jiang, H.; Li, Z. Global Mittag-Leffler stability and synchronization of discrete-time fractional-order delayed quaternion-valued neural networks. *Neurocomputing* **2022**, *511*, 290–298. [[CrossRef](#)]
32. Cai, X.; Shi, K.; She, K.; Zhong, S.; Kwon, O.; Tang, Y. Voluntary defense strategy and quantized sample-data control for T-S fuzzy networked control systems with stochastic cyber-attacks and its application. *Appl. Math. Comput.* **2022**, *423*, 126975. [[CrossRef](#)]
33. Qi, W.; Park, J.; Zong, G.; Cao, J.; Cheng, J. Synchronization for quantized semi-markov switching neural networks in a finite time. *IEEE Trans. Neural Netw. Learn. Syst.* **2021**, *32*, 1264–1275. [[CrossRef](#)]
34. Lu, B.; Jiang, H.; Hu, C.; Abudurahman, A.; Liu, M. H_∞ output synchronization of directed coupled reaction-diffusion neural networks via event-triggered quantized control. *J. Frankl. Inst.* **2021**, *358*, 4458–4482. [[CrossRef](#)]
35. Yang, X.; Cao, J.; Yang, Z. Synchronization of coupled reaction-diffusion neural networks with time-varying delays via pinning-impulsive controller. *SIAM J. Control Optim.* **2013**, *51*, 3486–3510. [[CrossRef](#)]
36. Tang, H.; Duan, S.; Hu, X.; Wang, L. Passivity and synchronization of coupled reaction-diffusion neural networks with multiple time-varying delays via impulsive control. *Neurocomputing* **2018**, *318*, 30–42. [[CrossRef](#)]
37. Shanmugam, L.; Mani, P.; Rajan, R.; Joo, Y. Adaptive synchronization of reaction-diffusion neural networks and its application to secure communication. *IEEE Trans. Cybern.* **2020**, *50*, 911–922. [[CrossRef](#)]
38. Chen, S.; Yang, J.; Li, Z.; Li, H.; Hu, C. New results for dynamical analysis of fractional-order gene regulatory networks with time delay and uncertain parameters. *Chaos Solitons Fractals* **2023**, *175*, 114041. [[CrossRef](#)]
39. Hu, X.; Wang, L.; Zhang, C.; Wan, X.; He, Y. Fixed-time stabilization of discontinuous spatiotemporal neural networks with time-varying coefficients via aperiodically switching control. *Sci. China Inf. Sci.* **2023**, *175*, 114041. [[CrossRef](#)]
40. Gu, Z.; Yue, D.; Ann, C.; Yan, S.; Xie, X. Segment-weighted information-based event-triggered mechanism for networked control systems. *IEEE Trans. Cybern.* **2023**, *53*, 5336–5345. [[CrossRef](#)]
41. Ge, X.; Han, Q.; Zhang, X.; Ding, D. Dynamic event-triggered control and estimation: A survey. *Int. J. Autom. Comput.* **2021**, *18*, 857–886. [[CrossRef](#)]
42. Luo, Y.; Yao, Y.; Cheng, Z.; Xiao, X.; Liu, H. Event-triggered control for coupled reaction-diffusion complex network systems with finite-time synchronization. *Phys. A Stat. Mech. Its Appl.* **2021**, *562*, 125219. [[CrossRef](#)]
43. Liu, L.; Bao, H. Event-triggered impulsive synchronization of coupled delayed memristive neural networks under dynamic and static conditions. *Neurocomputing* **2022**, *504*, 109–122. [[CrossRef](#)]
44. Jin, Y.; Qi, W.; Zong, G. Finite-time synchronization of delayed semi-markov neural networks with dynamic event-triggered scheme. *Int. J. Control Autom. Syst.* **2021**, *19*, 2297–2308. [[CrossRef](#)]
45. Vadivel, R.; Hammachukiattikul, P.; Gunasekaran, N.; Saravanakumar, R.; Dutta, H. Strict dissipativity synchronization for delayed static neural networks: An event-triggered scheme. *Chaos Solitons Fractals* **2021**, *150*, 111212. [[CrossRef](#)]
46. Selvaraj, P.; Kwon, O.; Lee, S.; Sakthivel, R. Equivalent-input-disturbance estimator-based event-triggered control design for master-slave neural networks. *Neural Netw.* **2021**, *143*, 413–424. [[CrossRef](#)]
47. Shanmugasundaram, S.; Udhayakumar, K.; Gunasekaran, D.; Rakkiyappan, R. Event-triggered impulsive control design for synchronization of inertial neural networks with time delays. *Neurocomputing* **2022**, *483*, 322–332. [[CrossRef](#)]
48. Cai, J.; Yi, C.; Wu, Y.; Liu, D.; Zhong, D. Leader-following consensus of nonlinear singular switched multi-agent systems via sliding mode control. *Asian J. Control* **2024**, 1–14. <https://doi.org/10.1002/asjc.3320>. [[CrossRef](#)]
49. Sun, Y.; Li, L.; Ho, D. Quantized synchronization control of networked nonlinear systems: Dynamic quantizer design with event-triggered mechanism. *IEEE Trans. Cybern.* **2023**, *53*, 184–196. [[CrossRef](#)]
50. Hu, C.; Jiang, H.; Teng, Z. Impulsive control and synchronization for delayed neural networks with reaction-diffusion terms. *IEEE Trans. Neural Netw. Learn. Syst.* **2010**, *21*, 67–81.
51. Arslan, E.; Vadivel, R.; Syed, A.M.; Arik, S. Event-triggered H_∞ filtering for delayed neural networks via sampled-data. *Neural Netw.* **2017**, *91*, 11–21. [[CrossRef](#)]
52. Dong, T.; Wang, A.; Zhu, H.; Liao, X. Event-triggered synchronization for reaction-diffusion complex networks via random sampling. *Phys. A Stat. Mech. Its Appl.* **2018**, *495*, 454–462. [[CrossRef](#)]
53. Zhou, J.; Lu, J.; Lü, J. Pinning adaptive synchronization of a general complex dynamical network. *Automatica* **2008**, *44*, 996–1003. [[CrossRef](#)]
54. Chen, W.; Luo, S.; Zhang, W. Impulsive synchronization of reaction-diffusion neural networks with mixed delays and its application to image encryption. *IEEE Trans. Neural Netw. Learn. Syst.* **2016**, *27*, 2696–2710. [[CrossRef](#)]
55. Luo, L.; Li, L.; Huang, W. Asymptotic stability of fractional-order Hopfield neural networks with event-triggered delayed impulses and switching effects. *Math. Comput. Simul.* **2024**, *219*, 491–504. [[CrossRef](#)]
56. Li, H.; Cao, J.; Jiang, H.; Alsaedi, A. Graph theory-based finite-time synchronization of fractional-order complex dynamical networks. *J. Frankl. Inst.* **2018**, *355*, 5771–5789. [[CrossRef](#)]

-
57. Li, L.; Cui, Q.; Cao, J.; Qiu, J.; Sun, Y. Exponential synchronization of coupled inertial neural networks with hybrid delays and stochastic impulses. *IEEE Trans. Neural Netw. Learn. Syst.* **2023**, 1–13. [[CrossRef](#)]
 58. Wu, Y.; Chen, S.; Zhang, G.; Li, Z. Dynamic analysis of a stochastic vector-borne model with direct transmission and media coverage. *AIMS Math.* **2024**, *9*, 9128–9151. [[CrossRef](#)]

Disclaimer/Publisher’s Note: The statements, opinions and data contained in all publications are solely those of the individual author(s) and contributor(s) and not of MDPI and/or the editor(s). MDPI and/or the editor(s) disclaim responsibility for any injury to people or property resulting from any ideas, methods, instructions or products referred to in the content.